



## Research articles

# Effects of biocompatible surfactants on structural and corresponding magnetic properties of iron oxide nanoparticles coated by hydrothermal process



Hakan Köçkar\*, Oznur Karaagac, Fatmahan Özel

Department of Physics, Balıkesir University, 10145 Balıkesir, Turkey

## ARTICLE INFO

## Keywords:

Tartaric acid  
Ascorbic acid  
Hydrothermal process  
Coating  
Superparamagnetic iron oxide nanoparticles

## ABSTRACT

Effect of the biocompatible surfactants; tartaric acid, ascorbic acid and a mixture of them on the properties of the superparamagnetic iron oxide nanoparticles (SPIONs) were investigated, separately. The SPIONs were functionalized via hydrothermal process. It was observed from X-ray diffraction (XRD) and transmission electron microscopy (TEM) analysis that the nanoparticles were iron oxide and their shapes were about spherical. And, the particle sizes of all samples were calculated to be less than 8 nm from the TEM images and XRD patterns. Fourier transform infrared spectra and thermogravimetric analysis (TGA) results displayed that all nanoparticles were effectively coated with the surfactants. According to the TGA curves, tartaric acid and ascorbic acid coatings percentages for the corresponding samples are 6.1 and 15.4% at the temperature range of 30–600 °C, respectively. For consequent magnetic analysis, vibrating sample magnetometer showed that all samples were superparamagnetic and saturation magnetizations,  $M_s$  were 71.1 and 69.5 emu/g for the nanoparticles coated with tartaric acid and ascorbic acid, respectively. Furthermore, for the first time, the SPIONs were coated with a mixture of tartaric and ascorbic acid. For that, the TGA showed 26.4% mass loss at the same temperature range and the  $M_s$  value was found to be 65.2 emu/g with a smaller particle size. In this study, it can be said that considerably high  $M_s$  values were obtained. The use of the surfactants during the hydrothermal process provides a good coating of the surface of nanoparticles and the process also increases the  $M_s$  with the sizes within superparamagnetic limit and therefore can have the potential to use in biomedical applications.

## 1. Introduction

Magnetic nanoparticles have found various important applications in the fields of electronics, catalysis, environment protection, targeted drug delivery, magnetic hyperthermia and magnetic resonance imaging (MRI) because of their distinctive properties [1]. Among these applications, uses of iron oxide nanoparticles focus on biomedical areas like magnetic hyperthermia, MRI, etc. For biomedical applications, small nanoparticles with high saturation magnetization and superparamagnetic behaviour are needed. The biocompatibility of the nanoparticles is also important to be used in biomedical areas. Many methods have been used to synthesize magnetic nanoparticles such as hydrothermal processing, co-precipitation, sol-gel processing, thermal decomposition, reverse micelle, etc. [1,2]. The methods used for the synthesis are effective on the structural and magnetic properties of the nanoparticles [3]. Nanoparticles have been coated with in situ and post synthesis methods in the literature [3]. In order to obtain the

nanoparticles with desired properties, appropriate synthesis technique and synthesis parameters for the intended application area should be selected. It is also essential to obtain biocompatible nanoparticles which can be useful in biomedical applications. Besides the desired properties for specific applications, magnetic nanoparticles, which are intended to be used for biomedically, need to have biocompatibility. Many biocompatible polymer coatings such as polyethylene glycol [4], chitosan [5] and dextran [6] were used to coat magnetic nanoparticles, however, the non-magnetic polymer coating may increase the particles size, reduce the magnetic core properties and hence limits the applications in various fields. Thus, it is important to select a biocompatible surfactant that is effective in adjusting the properties of the nanoparticles during the synthesis (in situ coating). In the case of biocompatible coating materials, tartaric acid (TA) and ascorbic acid (AA) were used as coating agents. The purpose of the coating is to control the size of the nanoparticles and have a biocompatible coating at the same time. The TA is anti-oxidant and biocompatible material. It is colourless,

\* Corresponding author at: Balıkesir University, Science and Literature Faculty, Physics Department, Balıkesir, Turkey.

E-mail addresses: [hkockar@balikesir.edu.tr](mailto:hkockar@balikesir.edu.tr) (H. Köçkar), [karaagac@balikesir.edu.tr](mailto:karaagac@balikesir.edu.tr) (O. Karaagac), [fatmahanzel@hotmail.com](mailto:fatmahanzel@hotmail.com) (F. Özel).

<https://doi.org/10.1016/j.jmmm.2018.11.053>

Received 22 June 2018; Received in revised form 7 November 2018; Accepted 7 November 2018

Available online 08 November 2018

0304-8853/ © 2018 Elsevier B.V. All rights reserved.

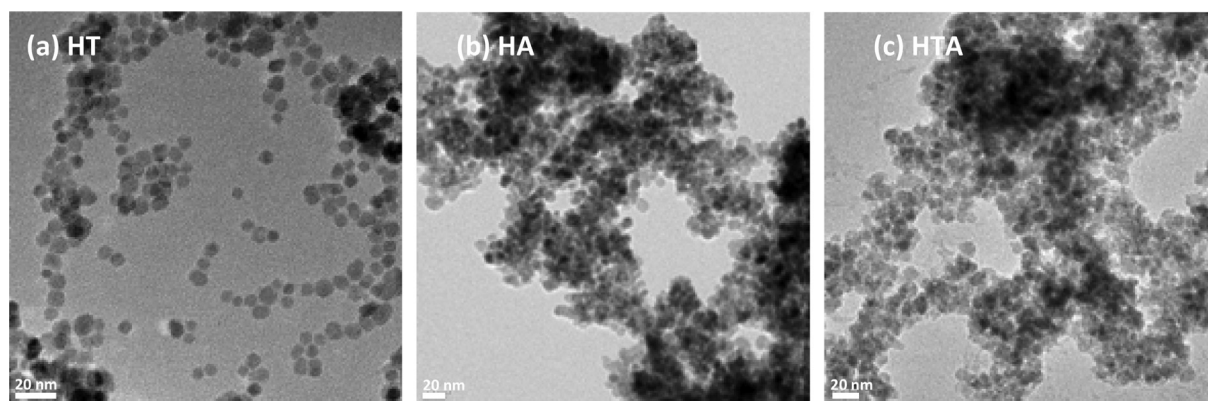


Fig. 1. TEM images of samples HT (a), HA (b) and HTA (c). The scale bars are nm for each image.

Table 1

The physical and magnetic properties of precursor and coated IONs.

Sample	Coating material	% coating	Magnetic properties		Particle sizes	
			$M_s$ (emu/g iron oxide)	$H_s$ (Oe)	$d_{TEM}$ (nm)	$d_{XRD}$ (nm)
HT	Tartaric acid	6.1	71.1	8042	$7.4 \pm 1.5$	9.4
HA	Ascorbic acid	15.4	69.5	8904	$7.8 \pm 1.7$	9.8
HTA	Tartaric acid and Ascorbic acid	26.4	65.2	7650	$6.8 \pm 2.0$	8.3

crystalline solid readily soluble in water and is widely used as acidulants in carbonated drinks, effervescent tablets, gelatin desserts, and fruit jellies [7]. As far as we are concerned, there are few studies [8,9] on the synthesis of TA coated iron oxide nanoparticles. Yan et al. [8] synthesized TA coated nanoparticles with the sizes of 10 nm and 15 nm via hydrothermal method, and the saturation magnetization of these nanoparticles were 29.6 and 40.1 emu/g, respectively. Scharlach et al. [9] modified the surface of iron oxide nanoparticles during the synthesis using different acids including TA and investigated the suitability for identification of atherosclerotic plaque. The AA (vitamin C) is also water soluble, biocompatible and anti-oxidant material. There are many reports [10–13] on the synthesis of AA coated magnetic nanoparticles. Also AA coated nanoparticles have the potential to be used in the magnetic resonance imaging. Sreeja et al. [10] and Xiao et al. [11] claimed that AA coated superparamagnetic nanoparticles were suitable as a contrast agent in MRI. Also, Feng et al. [12] used AA coated nanoparticles as adsorbent for arsenic removal and they suggested that AA coated nanoparticles had a great potential for heavy metal removal. Because of the advantages, iron oxide nanoparticles were coated with TA and AA separately by using hydrothermal synthesis. As far as we concerned, it is the first time that a mixture of TA and AA was also used to coat iron oxide cores for comparison.

In this study, the best method fitting to our research was hydrothermal process due to improve the crystallinity of the nanoparticles and thus improve their magnetic properties as well as coating them with biocompatible surfactants. In this study, the effects of surfactants (TA and AA) on the properties of iron oxide nanoparticles (IONs) coated by hydrothermal process were studied. IONs were also coated with a mixture of TA and AA and their properties were investigated. Particles size of all surfactant coated IONs are less than 8 nm. It is seen that the coatings prevents IONs from growing and exceeding the superparamagnetic size limit. Under study, the coated superparamagnetic nanoparticles have remarkably high saturation magnetization values (65.2–71.1 emu/g).

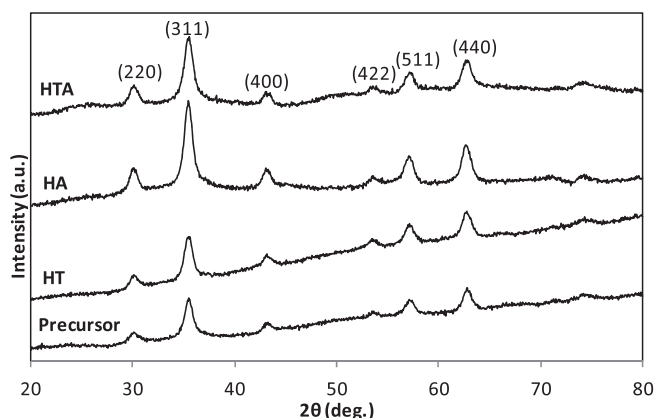


Fig. 2. XRD patterns of the precursor (a) and the samples HT (b), HA (c) and HTA (d).

## 2. Experimental

### 2.1. Materials

Ferrous chloride tetrahydrate ( $\text{FeCl}_2 \cdot 4\text{H}_2\text{O}$  Merck > 99%) ferric chloride hexhydrate ( $\text{FeCl}_3 \cdot 6\text{H}_2\text{O}$  Merck > 99%) and ammonium hydroxide ( $\text{NH}_4\text{OH}$  Merck, 25% of ammonia) were used for the synthesis of iron oxide nanoparticles. L (+) Ascorbic acid (Carlo Erba, 99%) and L (+) Tartaric Acid (Sigma-Aldrich,  $\geq 99.7$ ) were used as the coating agents. All chemicals were of reagent grade and used without further purification.

### 2.2. Synthesis of coated nanoparticles

Surfactant coated iron oxide nanoparticles were obtained via hydrothermal method by using TA, AA and a mixture of them during the hydrothermal synthesis. In order to prepare the precursor, the procedure in [14] was used. Briefly, 25 ml  $\text{NH}_4\text{OH}$  (25%) was added to 25 ml of aqueous solution containing a total 75 mmol of  $\text{FeCl}_2 \cdot 4\text{H}_2\text{O}$  and  $\text{FeCl}_3 \cdot 6\text{H}_2\text{O}$  at molar ratio of 1:1. The solution was stirred for 2 min at 700 rpm. The precursor was obtained at room temperature and in air atmosphere. After the synthesis of precursor, 6 ml of precursor and 9 ml TA solution were transferred to the Teflon-sealed autoclave. The autoclave was kept at 160 °C for 12 h during the synthesis and cooled naturally after the reaction. The products were collected by magnet and washed with distilled water. In order to obtain in powder form, the sample was dried at 60 °C overnight. The sample coated with TA was obtained and labelled as the sample HT. Other samples were also synthesized according to this recipe by using 9 ml AA solution and 9 ml AA and TA solutions in total whose samples were labelled accordingly as

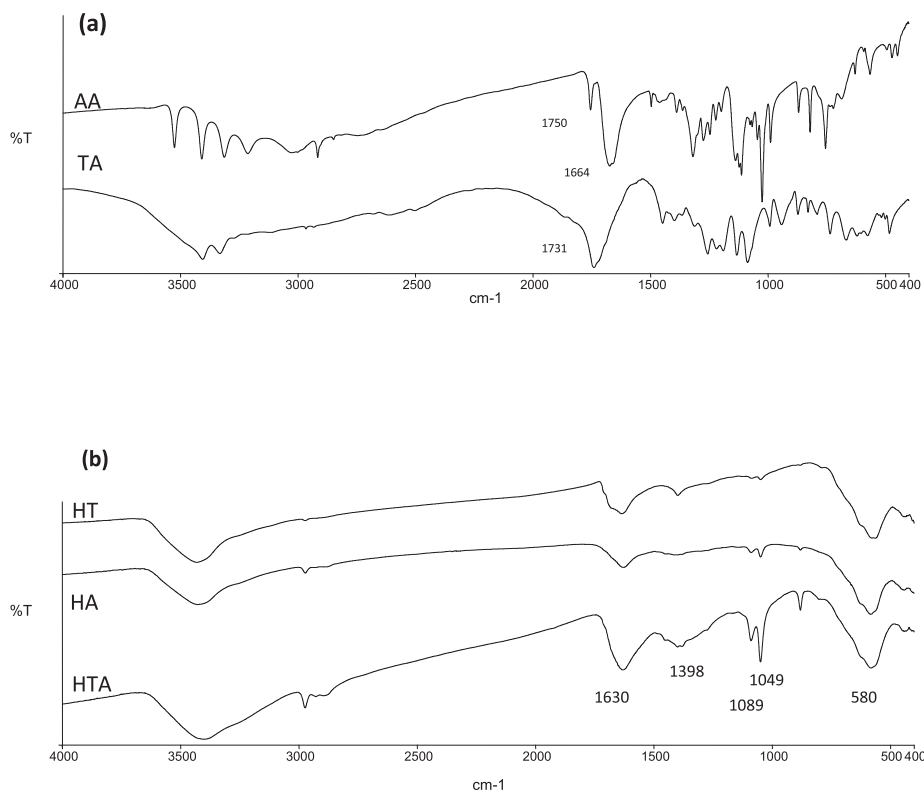


Fig. 3. FTIR spectra of ascorbic acid, tartaric acid (a) and the samples HT, HA and HTA (b).

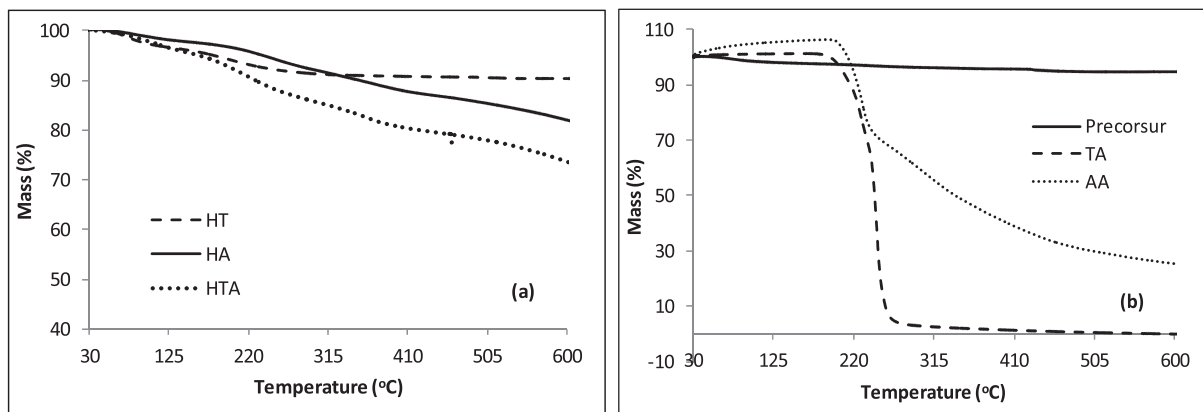


Fig. 4. TGA curves of the samples HT, HA and HTA (a) and Precursor, TA (tartaric acid) and AA (ascorbic acid) (b).

HA and HTA, respectively. The molar ratio of TA and AA is 1:1 for the synthesis of the nanoparticles coated with both AA and TA. In order to check nanoparticle stability against sedimentation by magnetic field gradients, the vessels were filled with the nanoparticle suspensions onto a strong permanent magnet and observed if a phase separation occurs during a few days. It is seen that all coated nanoparticles in water were well dispersed and also collected by the magnet.

### 2.3. Characterizations

Transmission electron microscopy (TEM) images were taken by an FEI Tecnai G2 F30 model scanning electron microscope. The samples were prepared by placing one drop of a dilute suspension of iron oxide nanoparticles in water on a carbon coated copper grid. The physical particle sizes were calculated from the TEM images by using ImageJ programme after taking the TEM pictures of nanoparticles. The phase purity and phase structure of the samples were investigated by the X-

ray powder diffraction (XRD) technique, using a PANalyticalX'Pert PRO X-ray diffractometer. The scan was performed between  $2\theta = 20-80^\circ$ . For the analysis of the Fourier transform infrared (FT-IR) spectra, samples were prepared as pellets by using KBr. The spectrum was recorded at  $400-4000\text{ cm}^{-1}$  by using Perkin-Elmer Spectrum Two spectrometer. Thermogravimetric Analysis (TGA) was performed by using Setaram TG-DTA-DSC. The heating rate was  $10^\circ\text{C}/\text{min}$  from 30 to  $600^\circ\text{C}$ . Argon was used as inert gas. Magnetic properties of powder samples were measured with ADE EV9 model vibrating sample magnetometer (VSM). Magnetic measurements were done at  $\pm 20\text{ kOe}$  with  $1\text{ Oe}$  intervals at room temperature. Saturation magnetization,  $M_s$  was calculated by using the maximum magnetization value measured within the applied fields. Saturation field,  $H_s$  was assumed as the field at which magnetization reaches  $0.95$  of  $M_s$  as given in the VSM system.

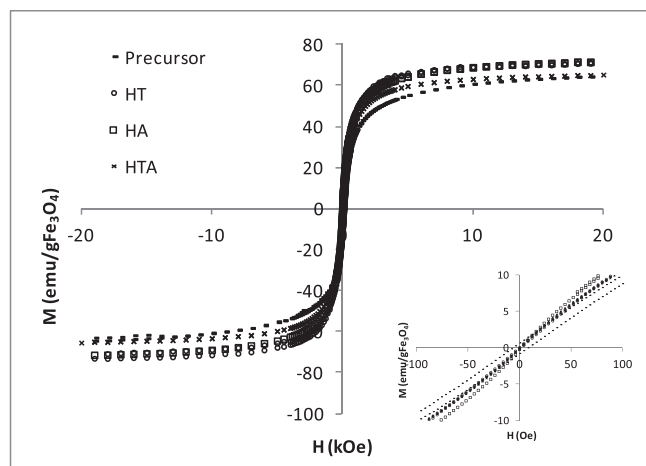


Fig. 5. Magnetization curves of precursor and the samples HT, HA and HTA. (Inset shows the magnetization curves at  $\pm 100$  Oe).

### 3. Results and discussion

TEM images of the coated nanoparticles were taken to determine the particles size and shape. The images of the samples HT, HA and HTA were given in Fig. 1a, b and c, respectively. TEM images of all samples show nearly spherical shaped nanoparticles. Besides, the dispersion of the sample HT maybe more favourable than the dispersions of HA and HTA since less agglomeration can be seen in the image (Fig. 1a). The mean physical sizes,  $d_{\text{TEM}}$  of the samples were calculated by using Image J and presented in Table 1. The  $d_{\text{TEM}}$  of the samples HT, HA and HTA are  $7.4 \pm 1.5$ ,  $7.8 \pm 1.7$  and  $6.8 \pm 2.0$  nm, respectively.

XRD measurements were carried out to characterize the crystalline structure of the precursor and the samples. The samples have the characteristic (2 2 0), (3 1 1), (4 0 0), (4 2 2), (5 1 1), (4 4 0) peaks of cubic spinel structure of magnetite (JCPDS no.019-0629) or maghemite (JCPDS no. 039-1346) as can be seen in the XRD pattern in Fig. 2. The precursor and all coated IONs show cubic spinel structure and no impurities were detected. The average crystal size,  $d_{\text{XRD}}$  of the samples HT, HA, HTA were calculated using Scherrer formula [15] and the crystal sizes were found to be 9.4, 9.8 and 8.3 nm, respectively, see Table 1. The  $d_{\text{XRD}}$  values are consistent with the  $d_{\text{TEM}}$  values. The particle sizes of the TA and AA coated nanoparticles are close to each other, however the size of the nanoparticles coated with a mixture of TA and AA is found to be smaller.

The synthesised nanoparticles were also characterized by the FT-IR spectroscopy and TGA analysis. The FT-IR spectrum of pure AA, TA and the coated IONs obtained by hydrothermal method were presented in Fig. 3. In the spectrum of AA in Fig. 3a, a series of bands at  $3519 \text{ cm}^{-1}$ ,  $3404 \text{ cm}^{-1}$ ,  $3306 \text{ cm}^{-1}$  and  $3209 \text{ cm}^{-1}$  are assigned to OH stretching in AA. The bands at  $1750 \text{ cm}^{-1}$  and  $1664 \text{ cm}^{-1}$  are assigned to C=O and C=C bonds, respectively [16]. In the spectrum of TA in Fig. 3a, a broad band including  $3404 \text{ cm}^{-1}$  and  $3325 \text{ cm}^{-1}$  peaks is attributed to O–H stretching. The band at  $1731 \text{ cm}^{-1}$  is assigned to the C=O stretching vibration [11]. FT-IR spectra of coated IONs are shown in Fig. 3b. A strong absorption band is observed at around  $580 \text{ cm}^{-1}$  which is corresponding to the Fe–O bond of iron oxide. The flexing vibration of hydroxyl group (–OH) can be observed between  $3100 \text{ cm}^{-1}$  and  $3600 \text{ cm}^{-1}$ . This band may result from the adsorbed  $\text{H}_2\text{O}$  molecules on the surface or –OH group of AA or TA. Two peaks at  $1625 \text{ cm}^{-1}$  and  $1398 \text{ cm}^{-1}$  indicate that AA or TA is bound to the surface of nanoparticles [13,17,18]. Absence of the peak around  $1700 \text{ cm}^{-1}$  proves that there is no free TA and AA [10]. IONs are successfully coated with the TA, AA and a mixture of TA and AA.

Fig. 4(a) shows TGA curves of the coated IONs. TGA measurements

of precursor (bare iron oxide nanoparticles), TA and AA were also conducted and given in Fig. 4(b). For pure TA and AA, thermal decomposition peaks appear at  $248^\circ\text{C}$  and  $230^\circ\text{C}$ , respectively. In the TGA curve of the sample HT, two mass losses are present. The first mass loss represents the loss of moisture in the sample and the second can be attributed to the thermal decomposition of TA. In the curve of sample HA, the decomposition takes place at around  $255^\circ\text{C}$  which is higher than the decomposition temperature of AA, indicating that the binding of AA to the iron oxide nanoparticles. The TGA curve of sample HTA also show similar decomposition behaviour. According to the TGA analysis, it can be concluded that the samples are successfully coated with the surfactants used. Sample HT, HA and HTA present 6.1, 15.4 and 26.4% mass losses at the temperature range of  $30\text{--}600^\circ\text{C}$ , respectively.

Magnetization curves of the coated IONs and uncoated (precursor) nanoparticles were shown in Fig. 5. Also, the  $M_s$  and  $H_s$  of the samples HT, HA and HTA were given in Table 1. Magnetic properties of coated IONs were measured and the  $M_s$  values were calculated due to the iron oxide core percentage obtained by TGA analysis. The  $M_s$  of the samples HT, HA and HTA are in the order of 71.1 emu/g, 69.5 emu/g and 65.2 emu/g, which are higher than the  $M_s$  of precursor (64.7 emu/g). For the most noticeable increase in  $M_s$  is seen in sample HT. The  $M_s$  of sample HT is 10% bigger than the  $M_s$  of precursor. The increase of  $M_s$  can be explained by the increase of crystallinity due to the high temperature synthesis conditions. The  $M_s$  of other samples also increases with hydrothermal process. The  $M_s$  values of coated IONs are consistent with the particle sizes as the  $M_s$  of HTA is lower than the that of HT and HA since the particle size of the sample HTA is smaller ( $6.8 \pm 2.0$  nm) than the sizes of HT and HA ( $7.4 \pm 1.5$  nm and  $7.8 \pm 1.7$  nm, respectively).  $M_s$  of magnetic nanoparticles increases with the increase of particle size as indicated in many studies [19,20]. The increase of  $M_s$  due to the increase of particle size is more appreciable in small nanoparticle as can be seen in [20], since the ratio of surface atoms to core atoms are bigger in small nanoparticles. Thus the increase of particle size reduces this ratio and gives a rise to the  $M_s$ . The  $H_s$  of the samples HT, HA and HTA are 8042, 8904 and 7650 Oe, respectively and  $H_s$  of the precursor is 11,168 Oe. The  $H_s$  values are much lower than that of the precursor indicating that it is easier to saturate the coated IONs than the precursor. The particles size of the precursor is around 9 nm. This value is under the superparamagnetic limit for iron oxide nanoparticles (25–30 nm) [21]. Therefore  $H_c$  value of the precursor seen in the inset of Fig. 5 is considered to be in the range of experimental errors. No  $H_c$  values are measured for the coated samples (HT, HA and HTA) at room temperature. Therefore, the coated samples were concluded as superparamagnetic in nature. The sample HT has a higher  $M_s$  than the TA coated nanoparticles (29.6 emu/g and 40.1 emu/g with  $H_c$ ) obtained in [8] with a smaller particle size and superparamagnetic nature. In the case of sample HA, better  $M_s$  than the AA coated nanoparticles (51 emu/g) in [11] and (40 emu/g) [12] with similar sizes and superparamagnetic behaviours were obtained. It is prevailed that the hydrothermal is a successful process for coating of IONs with current surfactants, preventing them from agglomeration and overgrowth and also enhancing the crystallinity and thus magnetic properties.

### 4. Conclusions

The effects of surfactants; tartaric acid, ascorbic acid and a mixture of them on the properties of iron oxide nanoparticles were investigated. The surface of the nanoparticles coated during the hydrothermal process prevented from exceeding the superparamagnetic size limit (the particle sizes are under 8 nm according to the TEM and XRD analysis). From the results of FTIR and TGA, the surface of nanoparticles was well-coated with surfactants. And a mixture of tartaric acid and ascorbic acid coated sample, which was for the first time used in this study, has the highest total surfactants mass on the surface of nanoparticles. All coated samples were superparamagnetic and their



saturation magnetization values were higher than that of precursor and varied depending on the type of surfactants used in the hydrothermal process. From the results, the nanoparticles coated with these biocompatible surfactants can potentially be used in biomedical applications. Therefore, further studies will be parameters optimisations of the current surfactant-coated nanoparticles with desirable properties to be effectively used in biomedical applications using SPIONs and other superparamagnetic ferrites i.e. cobalt ferrite, nickel ferrite and manganese ferrite.

## Acknowledgements

This work was supported by Balıkesir University, Turkey Research Grant no. BAP 2018/106. The authors would like to thank the State Planning Organisation, Turkey under Grant no 2005K120170 for VSM system. The authors also thank Physics Department, Balıkesir University for FT-IR and TGA analysis and the National Nanotechnology Research Center (UNAM), Bilkent University, Turkey for TEM and XRD analysis.

## References

- [1] A.H. Lu, E.L. Salabas, F. Schüth, Magnetic nanoparticles: Synthesis, protection, functionalization, and application, *Angew. Chem.* 46 (8) (2007) 1222–1244.
- [2] N.A. Frey, S. Peng, K. Cheng, S.H. Sun, Magnetic nanoparticles: synthesis, functionalization, and applications in bioimaging and magnetic energy storage, *Chem. Soc. Rev.* 38 (9) (2009) 2532–2542.
- [3] Z. Karimi, L. Karimi, H. Shokrollahi, Nano-magnetic particles used in biomedicine: Core and coating materials, *Mater. Sci. Eng. C-Mater. Biol. Appl.* 33 (5) (2013) 2465–2475.
- [4] S. García-Jimeno, J. Estelrich, Ferrofluid based on polyethylene glycol-coated iron oxide nanoparticles: characterization and properties, *Colloids Surf. A: Physicochem. Eng. Aspects* 420 (2013) 74–81.
- [5] S.-F. Shi, J.-F. Jia, X.-K. Guo, Y.-P. Zhao, D.-S. Chen, Y.-Y. Guo, T. Cheng, X.-L. Zhang, Biocompatibility of chitosan-coated iron oxide nanoparticles with osteoblast cells, *Int. J. Nanomed.* 7 (2012) 5593–5602.
- [6] A.M. Predescu, E. Matei, A.C. Berbecaru, C. Pantilimon, C. Drăgan, R. Vidu, C. Predescu, V. Kuncser, Synthesis and characterization of dextran-coated iron oxide nanoparticles, *R. Soc. Open Sci.* 5 (3) (2018) 171525.
- [7] J. Gawronski, K. Gawronska, Tartaric and Malic Acids in Synthesis, A source Book of Building Blocks, Ligands, Auxiliaries, and Resolving Agents, John Wiley & Sons Inc., USA, 1999.
- [8] J. Yan, S.B. Mo, J.R. Nie, W.X. Chen, X.Y. Shen, J.M. Hu, G.M. Hao, H. Tong, Hydrothermal synthesis of monodisperse Fe<sub>3</sub>O<sub>4</sub> nanoparticles based on modulation of tartaric acid, *Colloids Surf. A-Physicochem. Eng. Aspects* 340 (1–3) (2009) 109–114.
- [9] C. Scharlach, H. Kratz, F. Wiekhorst, C. Warmuth, J. Schnorr, G. Genter, M. Ebert, S. Mueller, E. Schellenberger, Synthesis of acid-stabilized iron oxide nanoparticles and comparison for targeting atherosclerotic plaques: Evaluation by MRI, quantitative MPS, and TEM alternative to ambiguous Prussian blue iron staining, *Nanomed.: Nanotechnol. Biol. Med.* 11 (5) (2015) 1085–1095.
- [10] V. Sreeja, K.N. Jayaprabha, P.A. Joy, Water-dispersible ascorbic-acid-coated magnetite nanoparticles for contrast enhancement in MRI, *Appl. Nanosci.* 5 (2015) 435–441.
- [11] L. Xiao, J. Li, D.F. Broughman, E.K. Fox, N. Feliu, A. Bushmelev, A. Schmidt, N. Mertens, F. Kiessling, M. Valldor, B. Fadeel, S. Mathur, Water-soluble superparamagnetic magnetite nanoparticles with biocompatible coating for enhanced magnetic resonance imaging, *ACS Nano* 5 (8) (2011) 6315–6324.
- [12] L. Feng, M. Cao, X. Ma, Y. Zhu, C. Hu, Superparamagnetic high-surface-area Fe<sub>3</sub>O<sub>4</sub> nanoparticles as adsorbents for arsenic removal, *J. Hazard. Mater.* 217–218 (2012) 439–446.
- [13] M. Aghazadeh, I. Karimzadeh, M.R. Ganjali, M.M. Morad, A novel preparation method for surface coated superparamagnetic Fe<sub>3</sub>O<sub>4</sub> nanoparticles with vitamin C and sucrose, *Mater. Lett.* 196 (2017) 392–395.
- [14] F. Ozel, H. Kockar, O. Karaagac, Growth of iron oxide nanoparticles by hydrothermal process: effect of reaction parameters on the nanoparticle size, *J. Supercond. Novel Magn.* 28 (2015) 823–829.
- [15] B.D. Cullity, Elements of X-ray Diffraction, Addison-Wesley, USA, 1978.
- [16] S.A.M.B. Dhasa, M. Suresh, G. Bhagavannarayana, S. Natarajan, Growth and characterization of L-Tartaric acid, an NLO material, *J. Cryst. Growth* 309 (1) (2007) 48–52.
- [17] H. Gupta, P. Paul, N. Kumar, S. Baxi, D.P. Das, One pot synthesis of water-dispersible dehydroascorbic acid coated Fe<sub>3</sub>O<sub>4</sub> nanoparticles under atmospheric air: Blood cell compatibility and enhanced magnetic resonance imaging, *J. Colloid Interface Sci.* 430 (2014) 221–228.
- [18] S.H. Xuan, L.Y. Hao, W.Q. Jiang, X.L. Gong, Y.A. Hu, Z.Y. Chen, Preparation of water-soluble magnetite nanocrystals through hydrothermal approach, *J. Magn. Mater.* 308 (2) (2007) 210–213.
- [19] G. Gnanaprakash, S. Mahadevan, T. Jayakumar, P. Kalyanasundaram, J. Philip, B. Raj, Effect of initial pH and temperature of iron salt solutions on formation of magnetite nanoparticles, *Mater. Chem. Phys.* 103 (2007) 168–175.
- [20] D. Makovec, A. Kosak, A. Znidarsic, M. Drogenik, The synthesis of spinel-ferrite nanoparticles using precipitation in microemulsions for ferrofluid applications, *J. Magn. Mater.* 289 (2005) 32–35.
- [21] K.M. Krishnan, Biomedical nanomagnetism: a spin through possibilities in imaging diagnostics, and therapy, *IEEE Trans Magn.* 46 (7) (2010) 2523–2558.